Kinetic Isomers of a Class II MHC−Peptide Complex†

Lutz Schmitt,‡ J. Jay Boniface,§ Mark M. Davis,§,|| and Harden M. McConnell*,‡

Department of Chemistry, Stanford University, Stanford, California 94305, Department of Microbiology and Immunology, Stanford University Medical School, Stanford, California 94305, and Howard Hughes Medical Institute, Stanford University Medical School, Stanford, California 94305

Received June 30, 1998; Revised Manuscript Received September 23, 1998

ABSTRACT: Class II major histocompatibility (MHC) molecules bind fragments of antigens and present them to T cells. The triggering of the T-cell receptor (TCR) of $CD4^+$ T-helper cells by these protein−peptide complexes is a key event in the generation of a cellular immune response. In the context of this interaction, it is generally assumed that class II MHC−peptide complexes adopt a single recognition structure at the cell surface. On the other hand, kinetic analysis has revealed that a number of class II MHC−peptide complexes show biphasic dissociation kinetics, indicating the presence of multiple kinetic isomers. Here, we demonstrate that a water-soluble version of the murine class II MHC molecule I-E^k complexed with an antigenic peptide derived from pigeon cytochrome *c* (PCC) displays monophasic as well as biphasic dissociation kinetics. While a simple monophasic dissociation curve was obtained at neutral pH, the complex showed biphasic dissociation behavior at acidic pH. This shift was independent of the ionic strength of the solution. Moreover, the short-lived isomer could be regenerated from a pool of kinetically homogeneous long-lived complexes. This demonstrates that the isomers interconvert and exist in a pH-sensitive equilibrium. Altering the peptide residue of PCC that occupies the P6 pocket of I-E^k results in a class II MHC−peptide complex that shows only monophasic dissociation, indicating that the glutamine at this position plays a key role in the kinetic heterogeneity of the complex.

Class II major histocompatibility (MHC)[1] molecules are α,β-heterodimeric transmembrane proteins which display protein fragments to the T-cell receptors (TCR) of $CD4^+$ T-helper cells. Only upon formation of a ternary class II MHC−peptide/TCR complex at the cell−cell interface is a cellular immune response generated against the presented peptide (reviewed in ref *1*). The formation and presentation of stable, long-lived class II MHC−peptide complexes are often assumed to be prerequisite for the activation of the TCR (*2*). As a consequence, these protein−peptide complexes might follow simple monophasic dissociation kinetics. However, over the past years a number of class II MHC−peptide complexes have been described which follow biphasic dissociation kinetics (*3*−*8*). In general, slow-dissociating (long-lived) complexes have lifetimes on the order of tens to hundreds of hours (*9*), whereas fast-dissociating (short-lived) complexes dissociate in minutes under physiological conditions (*8, 10, 11*).

While long-lived complexes are assumed to represent the immunologically relevant class II MHC−peptide complex, it has been suggested that short-lived complexes represent an intermediate in the generation of the long-lived complex (*3, 5*) or preserve the function of class II MHC proteins (*6*). There are also suggestions that short-lived complexes are involved in autoimmune diseases (*12*−*14*) or the escape from tolerance (*10*). Finally, it has been shown that both short- as well as long-lived class II MHC−peptide complexes can be specifically recognized by TCRs (*15*).

Structural information concerning the architecture of class II MHC−peptide complexes has been provided by X-ray crystallography (*16*−*20*). The most striking feature of existing crystal structures is the conservation of peptide conformation (*21*). Nevertheless, so far only the structures of long-lived class II MHC−peptide complexes have been solved. With regards to the differences in stability of long- versus short-lived complexes, it can be speculated that the structure of these kinetically less stable complexes might differ substantially from the reported high-resolution structures of class II MHC−peptide complexes. A first attempt to address this open question has been undertaken by combining experimental data and molecular-modeling approaches to predict the structure of a short-lived class II MHC−peptide complex (*22*).

Here, we show that short-lived class II MHC−peptide complexes can be generated from a pool of long-lived

† The Deutsche Forschungsgemeinschaft supported L.S. (Grant Schm 1279/1-1). The Irvington Institute of Medical Research supported J.J.B. This research was funded by the Howard Hughes Medical Institute (M.M.D.) and the National Institute of Health (H.M.M., Grant 5R37 AI13587-24).

* To whom correspondence should be addressed. Phone: +(650) 723-4571. Fax: +(650) 723-4943. E-mail: harden@leland.stanford.edu.

‡ Department of Chemistry.

§ Department of Microbiology and Immunology.

|| Howard Hughes Medical Institute.

[1] Abbreviations: C/P, 100 mM citrate/phosphate (9:1) buffer; F-PCC, fluorescein-labeled PCC; MHC, major histocompatibility complex; Hb, hemoglobin; HEPES, *N*-(hydroxyethyl)piperazine-*N*′-2-ethanesulfonic acid; HLA-DM, human leukocyte antigen DM; MCC, moth cytochrome *c*; MES, 2-(*N*-morpholino)ethanesulfonic acid; NHS, *N*-hydroxysuccinimidyl; NMP, *N*-methylpyrolidinone; PBS, phosphate buffered saline, 10 mM phosphate, 150 mM NaCl (pH 7.0 if not otherwise indicated); PCC, pigeon cytochrome *c*; TCR, T-cell receptor; TFA, trifluoroacetic acid; UV, ultraviolet. Single-letter abbreviations for amino acid residues used in this study are as follows: A, Ala; D, Asp; E, Glu; H, His; I, Ile; K, Lys; L, Leu; Q, Gln; R, Arg; T, Thr; Y, Tyr.

10.1021/bi9815593 CCC: $15.00 © 1998 American Chemical Society
Published on Web 11/21/1998

complexes. As a model system, we chose a water-soluble version of the murine class II molecule I-E^k (*23*) complexed with an antigenic peptide derived from pigeon cytochrome *c* (PCC) residues 89−104. Examining the dissociation kinetics of this immunogenic complex, we demonstrate that a switch in the dissociation kinetics occurs at acidic pH. While monophasic kinetics were observed at neutral pH, a second kinetic isomer with fast-dissociating characteristics was observed at slightly acidic pH. More important, short- and long-lived complexes interconvert and exist in a pH-sensitive equilibrium. By analyzing the pH dependence of the appearance of the fast-dissociating component, we were able to define structural prerequisites of the antigenic peptide sequence involved in the generation of the short-lived complex. These results allowed us to relate kinetic and structural details of short-lived class II MHC−peptide complexes.

MATERIALS AND METHODS

Preparation of Water-Soluble I-E^k. Water-soluble I-E^k was prepared as previously described (*24*). The protein was purified by immunoaffinity chromatography using the monoclonal antibody 14.4.4 immobilized to cyanobromide-activated Sepharose 4B (Pharmacia, Piscatawaj, NJ). After elution, I-E^k was concentrated into PBS (pH 7.4) by Centricon 30 ultrafiltration (Amicon, Heparia, CA) and stored at 4 °C at a concentration of approximately 2 mg/mL (28 μM). A molar extinction coefficient of 1.4×10^5 M cm^{-1} at 280 nm was used to calculate concentrations of I-E^k.

Peptide Synthesis. All peptides were synthesized on an Applied Biosystems 431A peptide synthesizer (Applied Biosystems, Foster City, CA) using standard Fmoc chemistry. For N-terminal fluorescence labeling after piperidine deprotection, resin was washed with NMP, methanol, and ether and dried under vacuum. The dry resin was suspended in DMSO containing a 5-fold molar excess of 5,6-NHS-carboxy fluorescein (Molecular Probes, Eugene, OR) and 2% (vol/vol) *N*-diisopropyl-ethylamine and allowed to react overnight in the dark at room temperature. The resin was washed, dried as above, cleaved, and deprotected for 3 h at room temperature in 90% TFA, 5% thioanisole, and 5% ethanedithiole (vol/vol). The cleaved and unprotected peptide was precipitated into ice-cooled *tert*-butyl methyl ether, dissolved in water/acetonitrile, and lyophilized. The crude peptide mixture was purified by reversed-phase chromatography on a Vydac RP_{18} column (5 μm, 4.6 × 25 cm) (Vydac, Beverly, MA) using an optimized water (0.1% TFA)/acetonitrile (0.1% TFA) gradient. Purified peptides were lyophilized, and identity was verified by high-resolution mass spectroscopy.

I-E^k/Peptide Complex Preparation. Water-soluble I-E^k (0.1 mg/mL) was incubated with a 30-fold molar excess of the corresponding fluorescein-labeled peptide (F-PCC) at 37 °C for 3 days in citrate/phosphate buffer (*25*), pH 5.3 (C/P), 150 mM NaCl, 1 mM PMSF, 1 μg/mL peptastin A, and 1 μg/mL leupeptin. The association reaction was then concentrated to approximately 0.4 mL by Centricon 30 ultrafiltration at 4 °C. The complex was purified by size-exclusion chromatography on a Sepharcyl S300HR column [30 × 1.5 cm (Pharmacia, Piscataway, NJ)] equilibrated with PBS (pH 7.4) and fractionated at a flow rate of 0.5 mL/min at 4 °C. Fractions corresponding to the class II MHC−peptide heterodimer were pooled and stored at 4 °C until further use. If the complex concentration was below 0.4 μM the protein was further concentrated using Centricon 30 ultrafiltration (Amicon, Heparia, CA) at 4 °C. Efficiency of complex formation was determined by the ratio of the absorption at 280 nm (MHC absorption) and 495 nm (fluorescein absorption). To correct the absorption at 280 nm for residual fluorescein, the measured absorption value was multiplied by 0.7. Molar extinction coefficients of 6×10^5 M cm^{-1} at 495 nm and 1.4×10^5 M cm^{-1} at 280 nm were used for the calculations.

HEPES/MES (H/M) Buffer System. A H/M buffer system was used in all dissociation experiments except as otherwise stated. This system guarantees a stable pH in the range 5.1−8.1 with negligible affinity for metal ions. The buffers consist of 20 mM of each HEPES and MES and the indicated amounts of NaCl. pH values were adjusted with concentrated HCl or NaOH.

Dissociation Experiments. For the dissociation experiments, F-PCC/I-E^k complex was diluted into room-temperature buffer with the indicated concentrations of NaCl in the presence of a 100-fold molar excess of unlabeled PCC (89−104) and incubated at 25 °C. The final complex concentration was 20 nM in all experiments. The presence of unlabeled competitor peptide was necessary to prevent rebinding of fluorescence-labeled PCC during the dissociation experiments. To determine the necessary concentrations, dissociation experiments were performed with varying concentrations of unlabeled PCC (89−104). Under all conditions, a 20-fold molar excess was sufficient to prevent rebinding. To provide a safe margin of error, all kinetic experiments were conducted in the presence of a 100-fold molar excess of competitor peptide. To avoid unspecific and irreversible adsorption of the PCC (89−104)/I-E^k complex to the incubation tubes, presiliconized tubes (ISC, Kaysville, UT) were used. At the indicated times, 20 μL aliquots were taken out and analyzed by high-performance size-exclusion chromatography (HPSEC) with a TosoHaas G3000SW column [0.75 × 60 cm (TosoHaas, Motgomeryville, PA)] and a TosoHaas guard column [0.75 × 7 cm (TosoHaas, Montgomeryville, PA)] connected to a fluorescence detector (Shimadzu RF-535). HPSEC separations were performed in PBS at room temperature at a flow rate of 1 mL/min. Fluorescence intensity was measured as the height of the signal corresponding to the $\alpha\beta$-heterodimer (elution volume, 15.8 mL). To compare different dissociation experiments, fluorescence intensities $F(t)$ were normalized to the fluorescence intensity at time zero (F_0). Kinetic data were analyzed by fitting to either a single-exponential model (eq 1),

$$F(t) = e^{-k_A t} \quad (1)$$

where $F(t)$ is the observed fluorescence signal at time t and k_A the rate constant, or a double exponential model (eq 2),

$$F(t) = A_0 e^{-k_A t} + (1 - A_0)\, e^{-k_B t} \quad (2)$$

where $F(t)$ is the observed fluorescence signal at time t, A_0 the fraction of fast dissociating complex at time zero, $(1 - A_0)$ the fraction of slow dissociating complex at time zero, and k_A and k_B the corresponding rate constants. The accuracy of each fit was generally larger than 99.6%.

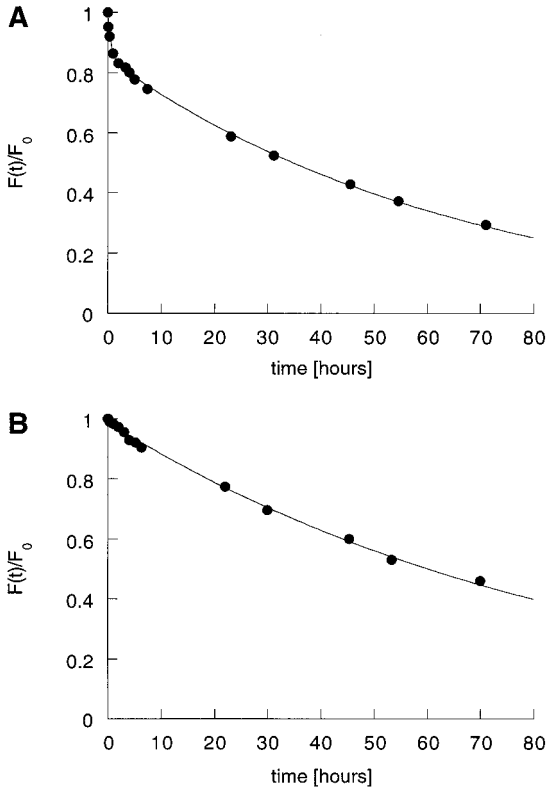

FIGURE 1: Dissociation kinetics of F-PCC (89−104)/I-E^k at (A) pH 7.0 (PBS) and (B) pH 5.3 (C/P, 150 mM NaCl) at 25 °C. Complexes were prepared as described in the Materials and Methods and diluted into the appropriate buffer. To avoid possible rebinding during the course of dissociation, a 100-fold molar excess of unlabeled PCC (89−104) was added. The dissociation shown in panel A was fitted to a monoexponential decay, whereas the dissociation shown in panel B was fitted to a biexponential decay. Kinetic parameters were as follows: (A) pH 7.0, $t_{1/2} = 51.2 \pm 1$ h; (B) pH 5.3: magnitude of fast-dissociating complex = 14.3% ± 0.9%, $t_{1/2} = 24.5 \pm 5$ min and magnitude of slow-dissociating complex = 85.7 ± 0.6%, $t_{1/2} = 49.6 \pm 0.2$ h. Each fit showed an accuracy of ≥99.8%. In both cases, fluorescence intensity was normalized to the complex intensity at time $t = 0$. Data points were collected until the fluorescence signal approached zero and were used in the fitting procedure, but are shown only up to 80 h.

Regeneration Experiment (Figure 5). A 100 mM citrate/phosphate (9:1) buffer system (C/P) was used in the regeneration experiment (Figure 5) for the dissociation at pH 5.3. This buffer system allowed the immediate drop in pH from 7.0 to 5.3 by addition of a calculated amount of 1 M citrate (pH 4.8) to the class II MHC−peptide sample in PBS (indicated for example by the second arrow in Figure 5). To raise the pH from 5.3 to 7.0 and remove already dissociated peptide, the remaining complex was isolated at 4 °C by Sephadex G50-SF (Pharmacia, Piscataway, NJ) gel filtration on a 2 mL disposable column equilibrated in PBS and pretreated with 1 mg/mL lysozyme to minimize non-specific binding, as indicated by the first arrow in Figure 5.

Molecular Modeling. The structures of the PCC (89−104) and PCC (89−104) Q100A/I-E^k complexes were modeled using the software package Look (Molecular Application Group, Palo Alto, CA) as described in Lee and McConnell (*26*). Coordinates of the hemoglobin Hb (68−76)/I-E^k complex (*19*) were used as a starting point for the alignment procedure (Brookhaven Protein Data Bank entry 1IEA).

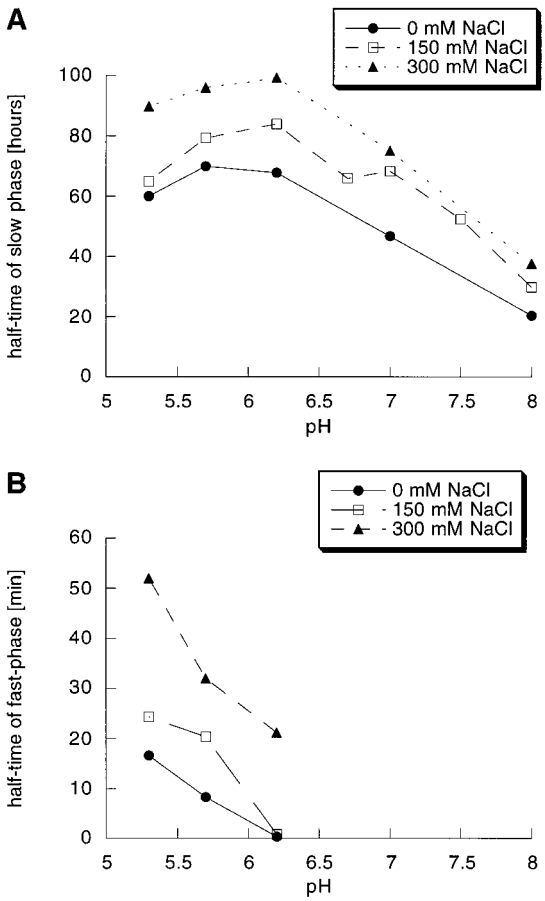

FIGURE 2: Half-times of the slow (A) and fast dissociating complex (B) of F-PCC (89−104)/I-E^k in dependence of salt and pH. All experiments were performed in H/M buffer at 25 °C in the presence of a 100-fold molar excess of unlabeled PCC (89−104). The obtained dissociation curves were fit to a biexponential decay for pH 5.3−6.2 and a monoexponential decay for pH 6.7 to pH 8.0 at all indicated salt concentrations. Fits showed an accuracy of ≥99.6%. Data points in panel B represent the average value of two independent experiments.

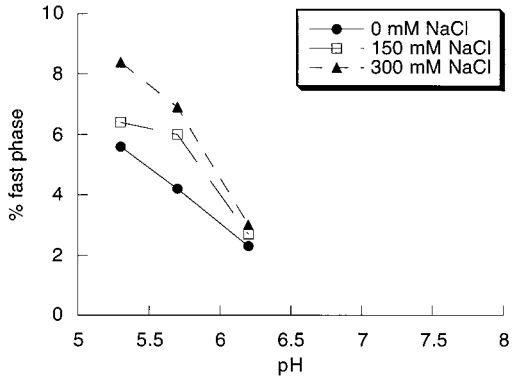

FIGURE 3: Percentage of fast-dissociating complex of the F-PCC (89−104)/I-E^k complex in dependence of pH and salt concentrations. Each dissociation experiment was performed in H/M, 25 °C in the presence of a 100-fold molar excess of unlabeled PCC (89−104) at the indicated salt concentrations. Fits showed an accuracy of ≥99.6%. Data points represent the average value of two independent experiments.

RESULTS

Fluorescein-labeled antigenic peptides derived from pigeon cytochrome *c* [(F-PCC (89−104), F-PCC (89−103), or the modified peptide F-PCC Q100A (89−104)] were used in

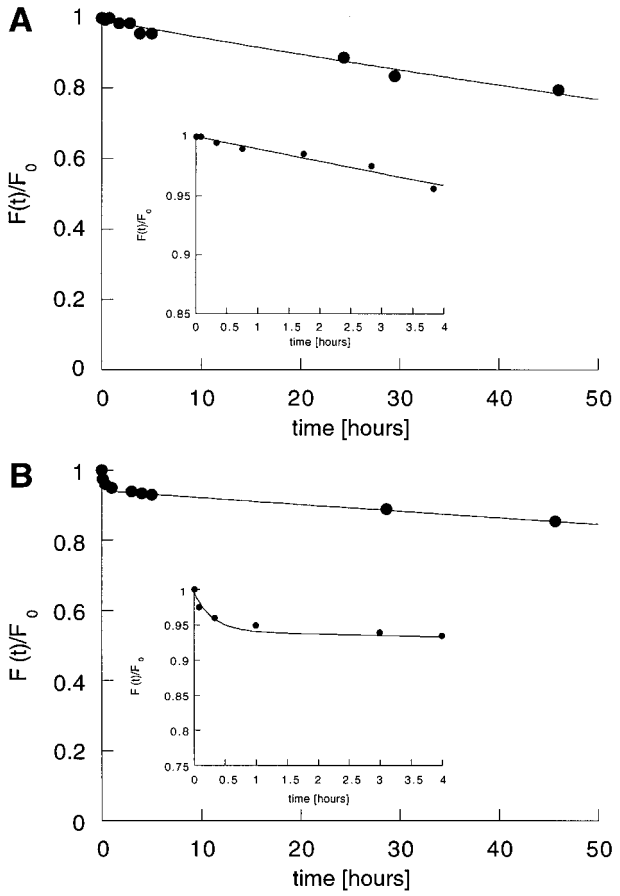

FIGURE 4: Dissociation kinetics of F-PCC (89−103)/I-E^k at 25 °C. Experiments were performed in H/M, pH 5.3, and 150 mM NaCl (A) and H/M, pH 7.0, and 150 mM NaCl (B) in the presence of a 100-fold molar excess of unlabeled PCC (89−104). Data points shown in panel A were fit to a monoexponential decay, and data points shown in panel B to a biexponential decay. Each fit showed an accuracy of ≥ 99.4%. The data points collected until the fluorescence signal had approached zero were used in the fitting procedure, but are only shown up to 100 h. Determined kinetic parameters are given in Table 2. The insets in panels A and B are given to highlight the first 4 h of the dissociation reaction.

this study. The sequence and the alignment of these peptides inside the MHC peptide binding cleft are given in Table 1. The water-soluble version of the murine class II MHC molecule I-E^k complexed with these peptides could be isolated using well-established protocols (*23*, *24*, *27*) (see Materials and Methods). Recovery of the protein was generally between 60 and 80% and efficiency of the association reaction larger than 95%. Complexes were stored at 4 °C and used for more than 4 weeks without any detectable changes in their dissociation kinetics. For all dissociation experiments, class II MHC−peptide complexes were diluted into the appropriate buffer at indicated pH values and ionic strengths in the presence of unlabeled PCC (89−104). Because the dilution factor was generally larger than 30, the influence of the storage buffer (PBS) was neglected. The presence of unlabeled competitor peptide was necessary to prevent rebinding of the labeled peptide during the course of dissociation at 25 °C. As reported by Reay et al. (*28*), rebinding was detectable at acidic pH, but negligible at neutral and basic pH (data not shown).

As shown in Figure 1, a shift in the dissociation kinetics of F-PCC (89−104)/I-E^k was observed between pH 7.0 (Figure 1A) and pH 5.3 (Figure 1B). The kinetics were

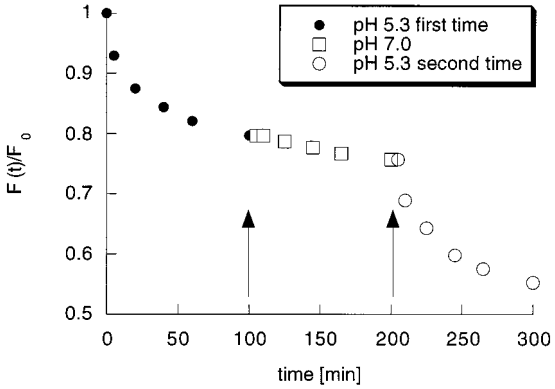

FIGURE 5: "Regeneration experiment". The dissociation of the F-PCC (89−104)/I-E^k complex was started in C/P, 150 mM NaCl in the presence of a 100-fold molar excess of unlabeled PCC (89−104) at 25 °C. At the time indicated by the first arrow, remaining complex was isolated by gelfiltration (see Materials and Methods). The concentration of the isolated complex was determined by UV spectroscopy at 495 and 280 nm (see Materials and Methods). During the isolation the pH was raised to 7.0. Dissociation was resumed in PBS and 25 °C in the presence of a 100-fold molar excess of unlabeled PCC (89−104). At the time indicated by the second arrow, the pH was dropped to 5.3 by addition of a calculated amount of 1 M citrate (pH 4.8).

monophasic at neutral pH, but followed a biphasic decay at acidic pH. To our knowledge, this is the first time that such a pH-induced shift in the dissociation behavior of a class II MHC−peptide complex was observed. Since the ionic strength of both buffers differs significantly, it is possible that ionic strength also contributes to the observed shift in the dissociation kinetics.

To examine the influence of pH and ionic strength on the dissociation kinetics of F-PCC (89−104)/I-E^k separately, we used a H/M buffer system (*24*). This system possesses a stable buffer capacity and constant ionic strength over the investigated pH range. A summary of the dissociation reactions between pH 5.3 and 8.0 with varying salt concentrations (0−300 mM NaCl) is given in Figure 2. Rate data for the dissociations at pH 5.3, 150 mM NaCl, and pH 7.0, 150 mM NaCl, are given in Table 2. For the slow-dissociating complex, a plot of $t_{1/2}$ versus pH at different concentrations of NaCl is shown in Figure 2A. Under all examined salt concentrations (0−300 mM NaCl), a bell-shaped curve of $t_{1/2}$ versus pH was observed with a maximum around pH 6.2. The complex showed a higher stability at acidic than basic pH. For example, $t_{1/2}$ was determined to be 20.4 h at pH 8.0 (0 mM NaCl). It then raised to 67.9 h at pH 6.2 (0 mM NaCl) and again dropped to 60 h at pH 5.3 (0 mM NaCl). This trend was found for all examined ionic strengths. At individual pH values, $t_{1/2}$ increased with increasing salt concentration (factor ≤ 2.5).

Results for the fast-dissociating complex are summarized in Figure 2B. This complex was first detected at pH 6.2. In all dissociation experiments above this pH value, there was no indication of a second component. As with the slow-dissociation complex, increased salt concentrations increased $t_{1/2}$ of the fast-dissociating component at all pH values (factor ≤ 3). On the other hand, pH showed a large influence on $t_{1/2}$ of the fast-dissociating complex. Determined values ranged from 3 min (pH 6.2, 150 mM NaCl) to 52 min (pH 5.3, 300 mM NaCl). A similar but not as pronounced effect of pH and ionic strength was observed for the magnitude of

Table 1

peptide−MHC							P1*	P2	P3	P4*	P5	P6*	P7	P8	P9*	
F-PCC (89-104)	A	E	R	A	D	L	I	A	Y	L	K	Q	A	T	A	K
F-PCC (89-103)	A	E	R	A	D	L	I	A	Y	L	K	Q	A	T	A	−
F-PCC (89-104) Q100A	A	E	R	A	D	L	I	A	Y	L	K	A	A	T	A	K

Table 2

peptide−MHC complex	pH	% fast-dissociating complex	$t_{1/2}$ (min)	% slow-dissociating complex	$t_{1/2}$ (h)
F-PCC (89-104)/I-E^k	5.3	6.0 ± 0.8	20.3 ± 10.1	94 ± 0.1	65.4 ± 0.9
	7.0	not observed	not observed	100	67.9 ± 1.0
F-PCC (89-103)/I-E^k	5.3	5.7 ± 1.2	18.6 ± 9.3	94.3 ± 0.7	330 ± 14.1
	7.0	not observed	not observed	100	223.6 ± 8.6
F-PCC (89-104) Q100A/I-E^k	5.3	not observed	not observed	100	28.9 ± 1.9

fast-dissociating complex (Figure 3). Increased ionic strength resulted in an increased amount of fast-dissociating complex (maximal change ≤ 1.5). This dependence on the ionic strength explains why only 6% of the fast-dissociating complex was observed for the H/M system at 150 mM NaCl (Figure 2B, Table 2), while 14% was determined for the C/P buffer (Figure 1B). The C/P buffer had a ionic strength of 0.5 M, whereas the H/M buffer had a ionic strength of 0.19 M (*24*). On the other hand, an increase in the magnitude of fast-dissociating component of a factor of 4 was observed for a decrease of pH from 6.2 (300 mM NaCl) to 5.3 (300 mM NaCl). More acidic pH values could not be employed, since dissociation of the MHC-heterodimer occurs below pH 5.0 (data not shown). Therefore, no experiments were performed below pH 5.3.

A possible explanation for the presence of a fast-dissociating complex might be drawn from the similarities between the sequences of the antigenic peptides derived from pigeon [PCC (89−104)] (Table 1) and moth cytochrome *c* (MCC 88−103) (*23*, *24*, *27*, *28*). Both peptides differ only in position 103. In the case of MCC (88−103), K103 is located in the P9 position. The corresponding residue in PCC (89−104) is A103. Furthermore, PCC (89−104) has an additional residue in P10 (K104). Therefore, it is possible that the two different kinetic states of PCC (89−104)/I-E^k correspond to different binding arrangements in the P9 pocket of I-E^k. In one situation, A103 may be bound to the P9 pocket, and in the other, K104. To investigate this hypothesis, we prepared the F-PCC (89−103)/I-E^k complex missing K104 (Table 1) and analyzed the dissociation kinetics at pH 7.0 and 5.3 (Figure 4 and Table 2). The same pH-dependent shift in the dissociation behavior that was seen for F-PCC (89−104) was also observed for the truncated F-PCC (89−103) peptide. At pH 7.0 (Figure 4A), a monophasic dissociation and, at pH 5.3 (Figure 4B), a biphasic dissociation were observed. Whereas magnitude and rate constants of the fast-dissociating complex are virtually identical with the wild-type system (Table 2), the slow-dissociating complex shows a slower off-rate at both pH values. This higher kinetic stability indicates that K104 has a destabilizing effect. Nevertheless, the observed kinetic properties of both MHC−peptide complexes rule out a role of K104 in the generation of the second, fast-dissociating complex at acidic pH.

To verify that the two kinetically different states of F-PCC (89−104)/I-E^k are an intrinsic property of the complex, we performed a sequential dissociation experiment (Figure 5). To be able to change the pH quickly and in a defined way, we employed the C/P buffer instead of the H/M buffer system used in the experiments shown in Figure 2 (Materials and Methods). The dissociation was started at pH 5.3 (Figure 5, filled circles). At the time indicated by the first arrow in Figure 5, the remaining complex was separated from dissociated peptide by gel filtration (Materials and Methods). The amount of fast-dissociating complex still present after 100 min of dissociation is 3.4% of its initial value or 0.4% absolute [based on a $t_{1/2}$ value of 24.5 min (Figure 1)]. Following isolation, a dissociation of the complex was resumed in PBS at pH 7.0 (Figure 5, open squares). Here, the expected monophasic behavior is observed. At 200 min, the pH of the sample was dropped to 5.3 by addition of an aliquot of 1 M citrate (pH 4.8) (Figure 5, second arrow). This dissociation again showed a biphasic decay (Figure 5, open circles). Both magnitude and off-rate of the fast-dissociating component are virtually identical to the first dissociation at pH 5.3. Thus, the fast-dissociating complex must have been regenerated at pH 7.0. The experiment further demonstrates that these two kinetic states of F-PCC (89−104)/I-E^k are in a pH-dependent equilibrium and that the appearance of two kinetic isomers is an intrinsic property of the complex (and is not due to protein heterogeneity).

While the regeneration experiment shown in Figure 5 demonstrated that both kinetic isomers interconvert, it is not clear whether they also interconvert at the same pH values. Therefore, we performed dissociation experiments with varying times for the association reaction (Figure 6). At the time indicated in Figure 6, the reaction between empty water-soluble I-E^k and F-PCC (89−104) was stopped and the formed class II MHC−peptide complex was separated from free peptide by gelfiltration on spin columns. Dissociations were started by diluting the isolated complex into C/P buffer, pH 5.3, and 150 mM NaCl, 100-fold molar excess of unlabeled competitor peptide and incubating the sample at 25 °C. As shown in Figure 6, the magnitude of fast-dissociating complex decreased by a factor of 3 over the range of association times. This demonstrates that both states of the F-PCC (89−104)/I-E^k complex are not only regenerated during a pH recycling (Figure 5) but also interconvert at pH 5.3 (Figure 6).

As shown in Figure 2B and Figure 3, the pH-dependent appearance of a fast-dissociating complex of F-PCC (89−104)/I-E^k resembles a titration curve with a 50% value around pH 6.0. Protein folding can induce a shift in the pK_A values of amino acids up to 2 pH units (*29*). Thus, this value corresponds roughly to the pK_A value of the side chains of

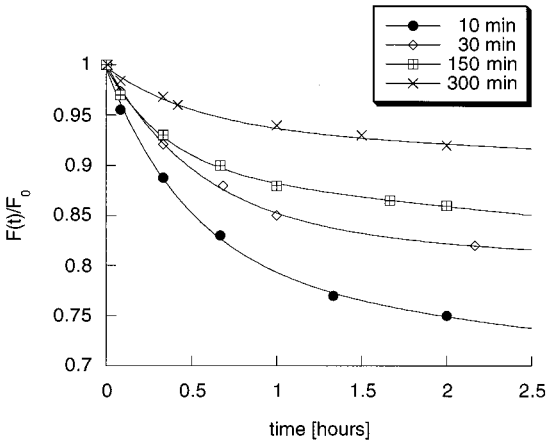

FIGURE 6: Dissociation kinetics of F-PCC (89−104)/I-E^k at 25 °C in dependence of incubation time. Water-soluble I-E^k was incubated with F-PCC (89−104) as described in the Materials and Methods. At the indicated times, F-PCC (89−104)/I-E^k complex was isolated and separated from free peptide at 4 °C by Sephadex G50-SF (Pharmacia, Piscataway, NJ) gelfiltration on a 2 mL disposable spin column equilibrated in PBS and pretreated with 1 mg/mL lysozyme. Concentration of the isolated class II MHC−peptide complex was determined at 280 nm (protein) and 495 nm (fluorescein) as described in the Materials and Methods. For the dissociation experiments, F-PCC (89−104)/I-E^k complex was diluted into C/P buffer, pH 5.3, and 150 mM NaCl and 100-fold molar excess of unlabeled PCC (89−104) to yield a final concentration of 20 nM. The experiment was started by incubating the sample at 25 °C. All dissociation experiments were fitted to a biexponential decay function.

H, E, or D. Inspection of the X-ray structure of I-E^k complexed with the antigenic peptide from hemoglobin Hb (64−76) (*19*) reveals the absence of H residues in the proximity of the complexed peptide. Consequently, only E11 and D66 of the α-chain that form the floor of the P6 pocket can account for the observed pH dependence. To investigate this, we analyzed the dissociation kinetics of the F-PCC Q100A (89−104)/I-E^k complex in which Q100 is substituted with A (Table 1) at pH 5.3 under all salt strengths (Figure 7A, no NaCl; B, 150 mM NaCl; C, 300 mM NaCl). This mutant contains a substitution of the peptide residue located at the P6 binding pocket of the I-E^k molecule. No fast-dissociating component was observed. This suggests that the interactions between the peptide residue in position 100 of PCC (89−104) and the residues forming the P6 binding pocket play an important role in the generation of kinetically different complexes. Moreover, the off-rate of the complex was reduced by a factor of 2 (Table 2). Although P6 is a minor binding pocket, the introduced mutation destabilizes the whole complex.

To relate our kinetic results to the X-ray structure of I-E^k (*19*), we created molecular models of the I-E^k peptide binding pocket P6 for the F-PCC (89−104)/I-E^k (Figure 8A) and F-PCC (89−104) Q100A/I-E^k (Figure 8B), respectively (see Materials and Methods). Both models are based on the high-resolution structure of I-E^k complexed with the antigenic peptide derived from hemoglobin [Hb (64−76)] (*19*) and were generated using the software package Look (Molecular Application Group, Palo Alto, CA) (*26*). In our model and in accordance with the Hb (64−76)/I-E^k structure, E11α, D66α, and Q100 are close enough (less than 3 Å) to favor the formation of a H-bonding network similar to the one determined for Hb (64−76)/I-E^k (Figure 8A). In the model

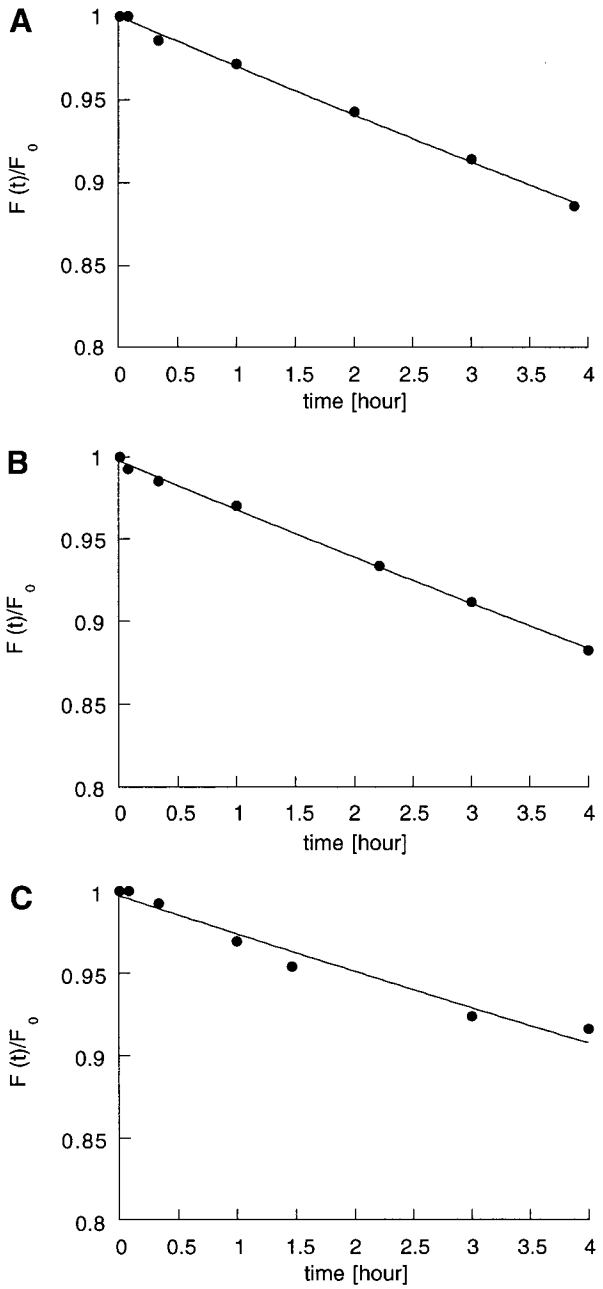

FIGURE 7: Dissociation kinetics of PCC (89−104) Q100A/I-E^k in H/M, pH 5.3, at 25 °C [(A) no NaCl, (B) 150 mM NaCl, and (C) 300 mM NaCl]. All dissociation curves were fitted to a single-exponential decay. The accuracy of all fits was ≥99.8%. To emphasize the strictly monophasic dissociation of this complex at all ionic strengths, dissociation curves are only shown up to 4 h, but data points were obtained until the fluorescence signal approached zero and were used to fit the data. Kinetic parameters for (B) are given in Table 2.

of the F-PCC (89−104) Q100/I-E^k complex, A100 is located at top of the binding pocket too far away (more than 5 Å) to interact directly with either one of the two acidic residues on the floor of the P6 pocket (Figure 8B). Thus, this missing interaction in the P6 pocket of the PCC (89−104) Q100A/I-E^k complex may explain the observed kinetic destabilization and the absence of a fast-dissociating complex.

DISCUSSION

The dissociation curves shown in Figure 1 demonstrate that the F-PCC (89−104)/I-E^k complex undergoes a shift in

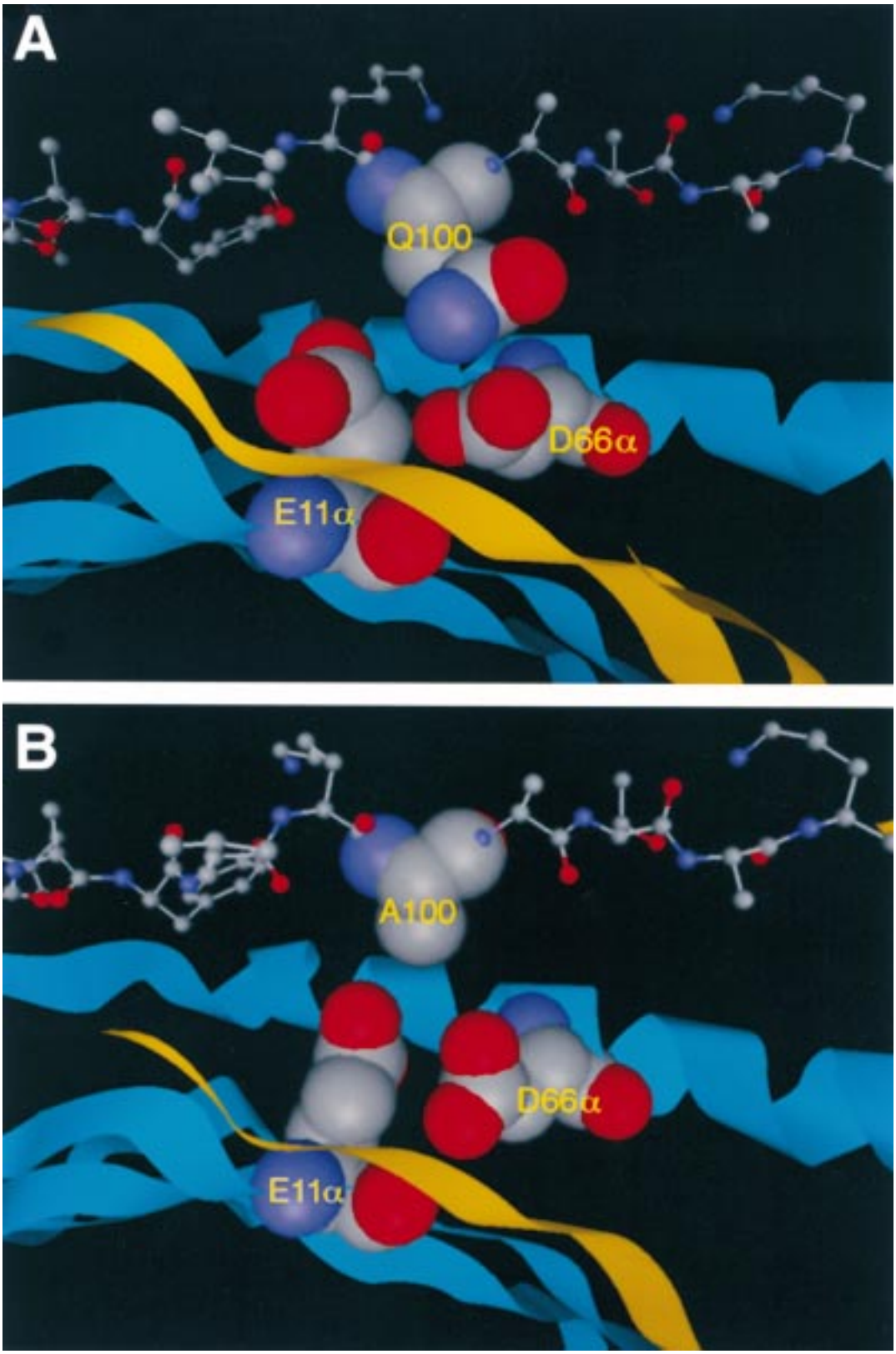

FIGURE 8: Structural models of residue Q100 of PCC (89−104)/I-E^k (A) and A100 of PCC (89−104) Q100A/I-E^k (B) located at the P6 binding pocket of the class II MHC molecule. Both structures were created based on the reported X-ray structure (*19*) of Hb (64−76)/I-E^k using the software package Look (see Materials and Methods). The two acidic residues on the floor of the P6 pocket (Eα66 and Dα11) as well as Q100 (panel A) and A100 (panel B) are shown in space filling representation (oxygen in red and nitrogen in blue) and parts of the antigenic peptide in wire-frame representation. The figure is arranged so that the viewer sees the architecture of the pocket from beneath the β-sheet forming the floor of the peptide binding groove of I-E^k. Also shown is the α-helix of the MHC α-chain forming the top of the peptide binding cleft. Q100 is in close contact with Eα66 and Dα11, forming a hydrogen-bond network between the amide moiety and the two carbon acids. A100 is located on top of the binding pocket. The distance between the methyl side chain and Eα66 and Dα11 prevents any direct interaction.

its dissociation kinetics with regards to pH. While a monophasic decay was observed at neutral pH (Figure 1A), the dissociation followed biphasic kinetics at pH 5.3 (Figure 1B). Due to the different ionic strengths of both buffers (PBS at pH 7.0 and C/P at pH 5.3), the contribution of ionic strength to the observed shift cannot be determined. We therefore employed a H/M buffer system (*24*). This system allowed the separation and quantification of pH and ionic strength effects. As summarized in Figure 2, the pH-induced shift was also observed for the H/M buffer system. At pH 6.7 and higher, only monophasic kinetics were obtained, whereas the dissociations at pH 6.2 and below were all biphasic. Thus, the observed shift is a pH-induced effect and is not due to changes in the salt concentration. Biphasic dissociations for class II MHC−peptide complexes have been described (*3*−7, *30*) and attributed for example to a preservation of functionality (*6*) or to an intermediate in the pathway to the final, immunologically active complex (*30*). But so far, no pH-induced switches within a single class II MHC−peptide complex have been observed.

The constant ionic strength of the H/M system enabled us to study the influence of salt concentration on the dissociation kinetics under defined pH conditions (Figure 2). For the slow-dissociating component (Figure 2A), a bell-shaped curve for $t_{1/2}$ versus pH with a maximum around pH 6.2 was determined. This kind of behavior was observed for all salt concentrations examined. The $t_{1/2}$ of the complex ranged from 20 h at pH 8.0 (0 mM NaCl) to 99.4 h at pH 6.2 (300 mM NaCl). Moreover, the F-PCC (89−104)/I-E^k complex showed a nearly identical stability at pH 5.3 and 7.0. While the same trend was observed for MCC (88−103)/I-E^k (*27*), all other class II MHC−peptide complexes described so far showed a significantly lower stability at acidic pH (*31*−*36*). It is therefore likely that this unusual pH dependence is a general property of the I-E^k molecule. In the case of the fast-dissociating complex, both half-time (Figure 2B) and magnitude of the fast-dissociating component (Figure 3) increased with increase of salt concentrations and decrease of pH. Under all conditions, the observed stabilization due to the increased ionic strength was within a factor of 2.5. Therefore, we believe that this trend results from a general stabilization of the protein by a more pronounced hydrophobic effect or a screening of electrostatic charges and not a specific, salt-dependent interaction between the antigenic peptide and the protein.

In summary, varying ionic strength influenced the dissociation kinetics of the F-PCC (89−104)/I-E^k complex in a general way whereas the pH displayed a pronounced, specific effect. This implies that an acidic environment alters the kinetic landscape of the dissociation reaction of this particular class II MHC−peptide complex in a fundamental way. The observed shift can be explained by the generation of a second kinetically distinguishable complex at acidic pH. On the other hand, it is possible that two kinetic isomers already exist at pH 7.0. If their off-rates were similar, the dissociation kinetics would still display a monophasic curve. An acidic pH might specifically destabilize one of the two isomers, thereby increasing its off-rate. As a result, the dissociation would follow a biexponential decay. On the basis of our results, both scenarios are possible.

Other studies using different approaches have described biphasic dissociation kinetics at neutral pH for this system (*3*, *4*). Sadegh-Naseri and McConnell (*3*) used PCC (88−104) and full-length I-E^k incorporated into a lipid bilayer and adsorbed to a glass slide. The different environment (lipid bilayer versus aqueous solution) and possible interaction between the surface and the MHC protein might induce structural changes in the protein. Such changes might form a second, kinetically distinguishable isomer at neutral pH. Furthermore, it is not clear if the employed system also displayed a kinetic heterogeneity at acidic pH. Witt and McConnell (*4*) studied the influence of temperature of the association reaction on the dissociation behavior of PCC (89−104) and full-length I-E^k. Only after an association reaction at low temperature, kinetic isomers were observed in the dissociation reaction at 37 °C and neutral pH. In comparison to our results, these findings demonstrate that the conditions of the association reaction can influence and even alter the kinetics of the dissociation reaction.

A comparison of the antigen epitopes of MCC (88−103) and PCC (89−104) reveals that they differ only in the peptide residue bound to the P9 pocket of I-E^k (K103 in the case of MCC and A103 in the case of PCC). The higher kinetic stability of MCC (*24*, *27*) and the presence of K104 in the PCC sequence located in the P10 position led us to speculate that different binding arrangements in the P9 pocket might be involved in the formation of a fast-dissociating complex. Accordingly, we examined the dissociation kinetics of the truncated F-PCC (89−103)/I-E^k at neutral pH (Figure 4A) and pH 5.3 (Figure 4B). An identical shift in the dissociation behavior was observed for the truncated system. Magnitude and half-time of the fast-dissociating component at pH 5.3 were virtually indistinguishable from the wild-type system (Table 2). Thus, a different binding arrangement of PCC (89−104) at the P9 position is not involved in the generation of a second kinetically distinguishable isomer at acidic pH.

To show that the pH-dependent shift of the kinetics of F-PCC (89−104)/I-E^k is an intrinsic property of the complex and not due to a second, low-affinity binding site (*37*) or an impurity of the protein sample, the regeneration experiment shown in Figure 5 was performed. Performing two dissociations at pH 5.3 separated by a dissociation at neutral pH resulted in the reappearance of the fast-dissociating isomer in the second dissociation at pH 5.3. Both magnitude and rate constant of the fast-dissociating complex were virtually identical. Due to the presence of a large molar excess of unlabeled competitor peptide, fluorescence-labeled F-PCC (89−104) dissociated during the dissociation at pH 5.3 or 7.0 cannot reassociate with empty I-E^k. Thus, a second binding site or protein heterogeneity can be eliminated as explanation for the fast-dissociating isomer. This shows that the pH-dependent presence of kinetic isomers is an intrinsic property of the protein and that the two complexes interconvert. It also indicates that the equilibrium or the interconversion rates between both isomers are sensitive to pH.

The dissociation kinetics of the F-PCC (89−104)/I-E^k complex examined for varying times of association between empty, water-soluble I-E^k and F-PCC (89−104) (Figure 6) demonstrated that the magnitude of fast-dissociating complex decreased as a function of association time. Consequently, both kinetically distinguishable complexes interconvert and the dissociation reaction of the F-PCC (89−104)/I-E^k complex at acidic pH follows one of the two reaction pathways outlined in reactions 3 and 4. Due to the presence

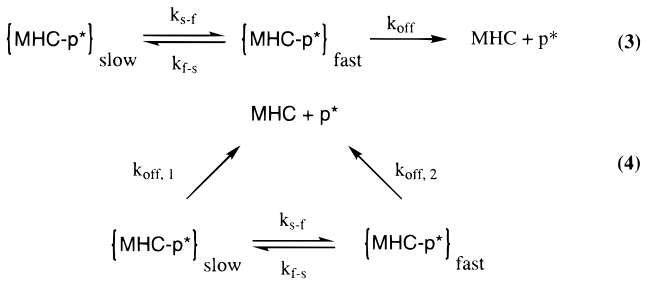

of a large molar excess of unlabeled competitor peptide, rebinding of dissociated fluorescence-labeled peptide is excluded in all experiments and is not shown in the reaction scheme.

In reaction 3, peptide dissociation involves an intermediate. The slow-dissociating complex can only dissociate after interconverting into the fast-dissociating complex. This mechanism has been proposed for the dissociation of PCC (88−104)/I-E^k incorporated in a lipid bilayer (*4*). Reaction 4 represents a parallel mechanism. The kinetic isomers dissociate independently from each other but also interconvert. Such a parallel mechanism but without interconversion of the two ligand−protein conformations has been observed for an antibody-combining side (*38)*. In case of the intermediate pathway (3), the association reaction does not proceed to equilibrium for short association times and the fast-dissociating complex becomes relatively more populated. This can result in a higher amount of detectable fast-dissociating complex. With prolonged association times, the thermodynamically less stable isomer interconverts into the slow-dissociating complex and the system reaches the equilibrium isomeric ratio. As a result, the magnitude of fast-dissociating complexes decreases with increased incubation times as seen in Figure 6. On the other hand, assuming a faster on-rate of the fast-dissociating complex in reaction 4, shorter incubation times would also lead to a higher occupancy of this complex. Only after prolonged incubation times, the kinetically more stable (slow-dissociating) complex becomes more populated by a direct binding reaction of peptide to empty, water-soluble I-E^k and interconversion from the fast-dissociating component. As a consequence, the magnitude of fast-dissociating component decreases with prolonged association times as seen in Figure 6. It is therefore not possible to distinguish conclusively between the two reaction pathways based on the observed results.

Assuming that the appearance of a fast-dissociating complex resembles a pH titration, the 50% value is around pH 6 under all salt concentrations (Figure 2B and 3). This implies that ionizable groups of I-E^k are involved in the generation of a second kinetic isomer. Inspection of the X-ray structure of Hb (64−76)/I-E^k (*19*) reveals that E11α and D66α are the only ionizable side chains located in proximity to the antigenic peptide. These two residues are conserved in all DR and I−E molecules and form the floor of the P6-binding pocket. The unexpected architecture of this MHC pocket where two acidic amino acids face each other has been discussed in detail by Fremont et al. (*19*). It has been suggested (*19*) that these two residues are the reason for the observed pH dependence of the association of antigenic peptides to I-E^k (*24*, *28*, *32*). If these residues are involved in the isomerism at acidic pH, introduction of an amino acid at position 100 of PCC that is unable to interact with these residues should eliminate one of the two kinetic isomers. As shown in Figure 7, substitution of Q100 with A100 resulted in monophasic dissociation kinetics of F-PCC (89−104) Q100A/I-E^k even at acidic pH. This shows that the protein residues forming the P6 pocket and the peptide side chain located at this position may indeed be responsible for the appearance of kinetically distinguishable isomers of the F-PCC (89−104)/I-E^k complex. Q100 forms a hydrogen network with the two acidic amino acid side chains on the floor of the P6 pocket (Figure 8A) and compensates for possible repulsive electrostatic forces between them. A100 on the other hand is located on top of this pocket too far away for any interaction (Figure 8B). This implies that an interaction between these three residues may be required for the generation of the fast-dissociating complex. The question remains whether the pH-dependent dissociation kinetics of the F-PCC (89−104)/I-E^k complex are based on a pH-sensitive isomerism of these three residues or a conformational isomerism of the protein itself. At pH 7.0, E11α and D66α are probably deprotonated and a formation of hydrogen bonds with the amide side chain of Q100 might compensate for the resulting electrostatic repulsion. At acidic pH, one or both of the acidic side chains of E11α and D66α are presumably protonated. As a result, the hydrogen bond network is weakened and dissociation facilitated. On the other hand, the I-E^k molecule is known to undergo a conformational change at acidic pH (*39*, *40*). If such a change influences the architecture of the P6 pocket, it could be transmitted to the peptide in the case of PCC (89−104). The missing interaction between A100 and the residues of the P6 pocket of PCC (89−104) Q100A would diminish any transmission of pH-dependent conformational changes of the protein.

It is tempting to speculate on the physiological relevance of the observed switch in the dissociation kinetics of F-PCC (89−104)/I-E^k. The acidic pH at which the fast-dissociating complex is detectable coincides with the apparent pH of the MHC class II loading compartment (*41*). One could therefore speculate that the presence of a less stable peptide conformation inside the peptide-binding cleft is essential for the catalytic function of HLA-DM in peptide exchange (*42*). Due to the observed interconversion of both isomers, peptide release would be accelerated. In the course of recycling of class II MHC−peptide complexes from the cell surface, antigenic epitopes can be exchanged (*43*). A fast-dissociating isomer that interconverts with the long-lived isomers would also accelerate this kind of exchange reaction. Although such physiological functions are speculative, more and more class II MHC−peptide complexes with biphasic dissociation kinetics have been described (*3*−*8*, *30*) and related to biological function (*6*, *15*). In combination with the results presented here, it seems likely that kinetic isomers of class II MHC−peptide complexes are of immunological importance.

ACKNOWLEDGMENT

We thank Thomas Anderson, Josh Rabinowitz, and Marija Vrljic for helpful suggestions and critical reading of the manuscript.

REFERENCES

1. Hedrick, S., and Edelmann, F. J. (1993) *Fundamental Immunology*, 3rd ed., Raven, New York.

2. Buus, S., Sette, A., Colon, S. M., Jenis, D. M., and Grey, H. M. (1986) *Cell 47*, 1071.
3. Sadegh-Nasseri, S., and McConnell, H. M. (1989) *Nature 338*, 274.
4. Witt, S. N., and McConnell, H. M. (1994) *Biochemistry 33*, 1861.
5. Beeson, C., and McConnell, H. M. (1994) *Proc. Natl. Acad. Sci. U.S.A. 91*, 8842.
6. Sadegh-Naseri, S., Stern, L. J., Wiley, D. C., and Germain, R. N. (1994) *Nature 370*, 647.
7. Mason, K., and McConnell, H. M. (1994) *Proc. Natl. Acad. Sci. U.S.A. 91*, 12463.
8. Mason, K., Denney, D. W., and McConnell, H. M. (1995) *J. Immunol. 154*, 5216.
9. Rothbard, J. B., and Gefter, M. L. (1991) *Annu. Rev. Immunol. 9*, 52.
10. Fairchild, P. J., Wildgoose, R., Atherton, E., Webb, S., and Wraith, D. C. (1993) *Int. Immunol. 5*, 1151.
11. Mason, K., Denney, D. W., and McConnell, H. M. (1995) *Biochemistry 34*, 14874.
12. Carrasco-Marin, E., Shimizu, J., Kanagawa, O., and Unanue, E. R. (1996) *J. Immunol. 156*, 450.
13. Joosten, I., Wauben, M. H. M., Holewijn, M. C., Reske, K., Pederson, L. O., Roodenboom, C. F. P., Hensen, E. J., van Eden, W., and Buus, S. (1994) *Int. Immunol. 6*, 751.
14. Zamvil, S. S., Mitchell, S. S., Moore, A. C., Kitamura, K., Steinmann, L., and Rothbard, J. B. (1986) *Nature 324*, 258.
15. Rabinowitz, J. D., Liang, M. N., Tate, K., Lee, C., Beeson, C., and McConnell, H. M. (1997) *Proc. Natl. Acad. Sci. U.S.A. 94*, 8702.
16. Brown, L. H., Jardetzky, T. S., Gorga, J. C., Stern, L. J., Urban, R. G., Strominger, J. L., and Wiley, D. C. (1993) *Nature 364*, 33.
17. Jardetzki, T. S., Brown, J. H., Gorga, J. C., Stern, L. J., Urban, R. G., Chi, Y.-I., Stauffacher, C., Strominger, J. L., and Wiley, D. C. (1994) *Nature 368*, 711.
18. Gosh, P., Amaya, M., Mellins, E., and Wiley, D. C. (1995) *Nature 378*, 457.
19. Fremont, D. H., Hendrickson, W. A., Marrack, P., and Kappler, J. (1996) *Science 272*, 1001.
20. Dessen, A., Lawrence, M., Cupo, S., Zaller, D. M., and Wiley, D. C. (1997) *Immunity 7*, 473.
21. Jardetzky, T. S., Brown, J. H., Gorga, J. C., Stern, L. J., Urban, R. G., Strominger, J. L., and Wiley, D. C. (1996) *Proc. Natl. Acad. Sci. U.S.A. 93*, 734.
22. Lee, C., Liang, M. N., Tate, K. M., Rabinowitz, J. D., Beeson, C., Jones, P. P., and McConnell, H. M. (1998) *J. Exp. Med. 187*, 1505.
23. Wettstein, D., Boniface, J. J., Reay, P. A., Schild, H., and Davis, M. M. (1991) *J. Exp. Med. 174*, 219.
24. Boniface, J. J., Albritton, N. L., Reay, P. A., Kantor, R. M., Stryer, L., and Davis, M. M. (1993) *Biochemistry 32*, 11761.
25. McIlvaine, T. C. (1921) *J. Biol. Chem. 49*, 183.
26. Lee, C., and McConnell, H. M. (1995) *Proc. Natl. Acad. Sci. U.S.A. 92*, 8269.
27. Reay, P. A., Kantor, R. M., and Davis, M. M. (1994) *J. Immunol. 152*, 3946.
28. Reay, P. A., Wettstein, D. A., and Davis, M. M. (1992) *EMBO J. 11*, 2829.
29. Schulz, G. E., and Schirmer, R. H. (1979) *Principles of protein structure*, Springer-Verlag, New York, Berlin, Heidelberg, Tokio.
30. Beeson, C., Anderson, T. G., and McConnell, H. M. (1996) *J. Am. Chem. Soc. 118*, 977.
31. Harding, C. V., Roof, R., W., Allen, P. M., and Unanue, E. R. (1991) *Proc. Natl. Acad. Sci. U.S.A. 88*, 2740.
32. Jensen, P. E. (1990) *J. Exp. Med. 171*, 1779.
33. Mouritsen, S., Hansen, A. S., Petersen, B. L., and Buus, S. (1992) *J. Immunol. 148*, 1438.
34. Sette, A., Southwood, S., O'Suillivan, D., Gaeta, F. C. A., Sidnay, J., and Grey, H. M. (1992) *J. Immunol. 148*, 844.
35. Tampé, R., and McConnell, H. M. (1991) *Proc. Natl. Acad. Sci. U.S.A. 88*, 4661.
36. Witt, S. N. and McConnell, H. M. (1991) *Proc. Natl. Acad. Sci. U.S.A. 88*, 8164.
37. Tompkins, S. M., Moore, J. C., and Jensen, P. E. (1996) *J. Exp. Med. 183*, 857.
38. McConnell, H. M., and Martinez-Yamout, M. (1996) *Adv. Protein Chem. 49*, 135.
39. Boniface, J. J., Lyons, D. S., Wettstein, D. A., Allbritton, N. L., and Davis, M. M. (1996) *J. Exp. Med. 183*, 119.
40. Runnels, H. A., Moore, J. C., and Jensen, P. E. (1996) *J. Exp. Med. 183*, 127.
41. Tulp, A., Verwoerd, D., Dobberstein, B., Ploegh, H., and Pieters, J. (1994) *Nature 369*, 120.
42. Sloan, V. S., Cameron, P., Porter, G., Gammon, M., Amaya, M., Mellins, E., and Zaller, D. M. (1995) *Nature 375*, 802.
43. Pinet, V., Vergelli, M., Martin, R., Bakke, O., and Long, E. O. (1995) *Nature 375*, 603.

BI9815593